Key Points:
- The decrease in NWC signal amplitude was observed at all five stations associated with 22 July 2009 total solar eclipse
- LWPC modeling showed an increase in the D region reflection height of about 2.3-3.0 km at stations under varying eclipse conditions
- The decrease in electron density varied from 58% to 71% in the region from near central line of totality to region on the fringe of totality

Correspondence to:
R. Singh,
rajeshsing03@gmail.com

The 22 July 2009 Total Solar Eclipse: Modeling D Region Ionosphere Using Narrowband VLF Observations

K. Venkatesham[1] (iD), Rajesh Singh[1] (iD), Ajeet K. Maurya[2] (iD), Adarsh Dube[1] (iD), Sushil Kumar[3] (iD), and D. V. Phanikumar[4]

[1]KSK Geomagnetic Research Laboratory, Indian Institute of Geomagnetism, Allahabad, India, [2]Department of Physics, Doon University, Dehradun, India, [3]School of Engineering and Physics, The University of the South Pacific, Suva, Fiji, [4]Aryabhatta Research Institute of Observational Sciences, Nainital, India

Abstract We present D region ionospheric response to 22 July 2009 total solar eclipse by modeling 19.8-kHz signal from NWC very low frequency (VLF) navigational transmitter located in the Australia. NWC VLF signal was received at five stations located in and around eclipse totality path in the Indian, East Asian, and Pacific regions. NWC signal great circle paths to five stations are unique having eclipse coverage from no eclipse to partiality to totality regions, and the signal is exclusively confined in the low and equatorial regions. Eclipse-induced modulations in NWC signal have been modeled by using long-wave propagation capability code to obtain D region parameters of reflection height (H') and sharpness factor (β). Long-wave propagation capability modeling showed an increase in H' of about 2.3 km near central line of totality, 3.0 km in the region near to totality fringe, and 2.4 to 3.0 km in the region under partial eclipse. Using H' and β, Wait ionosphere electron density (N_e) profile at the daytime altitude of 75 km showed a decrease in N_e by about 58% at a station near totality central line, whereas at totality fringe and in partial eclipse region decrease in the N_e was between 63% and 71% with respect to normal time values. The eclipse associated variations in the H', β, and N_e are less in low-latitude region as compared to midlatitude. The study contributes to explain observations of wave-like signature in the D region during an eclipse and difference in the eclipse effect in the different latitude-longitude sectors.

Plain Language Summary The work was taken up in light of recent 21 August 2017 great American total solar eclipse. An eclipse in magnitude larger than American eclipse happened on 22 July 2009 in Asia and Pacific region. We revisited our acquired very low frequency data to understand its effect on the ionized part of our upper space environment *ionosphere*, in low-latitude region as 22 July 2009 eclipse happened in low-latitude region. We performed long-wave propagation capability modeling on the observed very low frequency transmission and compared results with the great total eclipse in midlatitude to high-latitude regions. The results are unique and new and show that total eclipses have varied effect on D region ionosphere in different latitude-longitude sectors of the globe. The unique results obtained show that for an eclipse in low latitudes, the variations in H' and β are more and D region N_e reduction is less, when compared with eclipse in midlatitude region. Study contributes to explain observations of wave-like signature in ionosphere during eclipse and difference in eclipse effect on ionosphere in different latitude-longitude sector.

1. Introduction

A total solar eclipse (TSE) is known commonly to occur when dark shadow of the Moon totally obscures the intense bright daylight of the Sun on the Earth's surface. Any TSE attracts huge attention of the scientific community since it provides rare opportunity to understand the variability of various regions of the Earth's upper space environment during sudden absence of the solar ionizing radiation. A TSE is of particular interest to ionospheric radio science community because it is only during a TSE that the ionospheric electron density concentration is sharply reduced to a level close to nighttime values. Consequently, a TSE can severely affect radio communication supported by the ionosphere and can produce an error in the satellite navigation (Singh et al., 2011; Smith, 1972).

Under normal conditions, Sun's flux in the extreme ultraviolet and ultraviolet electromagnetic spectrum is a major source of ionospheric ionization (Hargreaves, 1992). But during a TSE, reduction in the solar
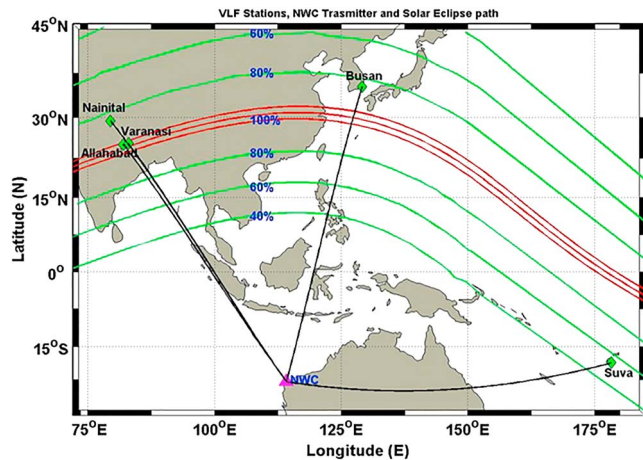
Figure 1. Representation of 22 July 2009 path of solar eclipse totality. The eclipse started in India (~00:51:00 UT) and ended in Pacific Ocean (~04:20:00 UT). The green diamonds show locations of very low frequency (VLF) receiving sites (Allahabad, Varanasi, Nainital, Busan, and Suva). The pink triangle shows the location of NWC (19.8 kHz) VLF transmitter in Australia.

flux leads to an abrupt reduction of ionospheric ionization. This ionospheric ionization variability is more noticeable in lower part of the ionosphere (D region). In the D region primary source of ionization during daytime is Sun's Lyman-α (1,215 Å) emission (Hargreaves, 1992). But due to blockage of Lyman-α radiation during TSE, the electron density of D region ionosphere is decreased considerably reaching to a value little higher than that at the nighttime (Smith, 1972). Very low frequency (VLF: 3–30 kHz) radio waves propagate hundreds of kilometers via multiple reflections in the Earth-ionosphere waveguide (EIWG) created by boundaries of conducting terrestrial ground surface and bottom of the D region ionosphere.

It is well known that D region because of its elevation range (daytime: ~60–75 km; nighttime 75–95 km) and low electron density remains the least studied region (Cummer & Inan, 2000; Hargreaves, 1992) of the ionosphere. The continuous investigation of the D-region is not possible using conventional methods such as balloon probes, ionosonde, or satellites from the top. Rockets and radars are not preferred for day-to-day or diurnal probing of D region due to their high cost of operation (Cummer & Inan, 2000). The VLF waves from fixed frequency transmitters make perfect tool to study lower part of the ionosphere (D region) very efficiently (e.g., Maurya et al., 2012, 2014, 2018).

The implications of TSE on ionosphere depend on various factors such as geophysical conditions, latitude, longitude, and local time of the SE occurrence (Baran et al., 2003; Maurya et al., 2018). Since past several decades, TSEs' studies using VLF waves have given episodically chances to study D region ionosphere. There are reports on the D region studies by using VLF observations during several TSEs (e.g., Clilverd et al., 2001; Guha et al., 2010, 2012; Kumar et al., 2016; Maurya et al., 2014; Ohya et al., 2012; Phanikumar et al., 2014; Reeve & Rycroft, 1972; Singh et al., 2012, 2011). But still, studies are limited because of the rare occurrence of TSEs. Eclipse effect on VLF signal propagation is local time and transmitter-receiver path length dependent, and for this reason every ionospheric study to explain TSE ramifications on the D region needs to have data recorded covering a vast region around a TSE path.

In this study, we have investigated the effect of 22 July 2009 TSE (the longest totality time TSE of the century) on D region ionosphere at low-equatorial latitudes in the Asia-Pacific region through observations and modeling of NWC VLF signal. Prior to this report, an extensive modeling of the D region during 11 August 1999 TSE using VLF observations at multiple sites was carried out by Clilverd et al. (2001) in the European sector, which covered midlatitude to high-latitude region. There are some studies on 22 July 2009 TSE effects using both broadband (300 Hz to 30 kHz) and narrowband (fixed frequency) VLF signal observations (e.g., Guha et al., 2010; Kumar et al., 2016; Ohya et al., 2012; Phanikumar et al., 2014; Singh et al., 2011; Zhang et al., 2011). But none of these studies was focused on modeling of D region ionosphere using a comprehensive data set from multiple sites covering whole eclipse region from the start of eclipse totality in India to its end in the Pacific Ocean. To fill this gap, we carried out modeling of D region ionosphere during 22 July 2009 TSE using NWC (19.8 kHz) VLF transmitter signal recorded at five receiver stations located in the total/partial eclipse conditions in India, South Korea, and Fiji. The respective transmitter and receiver locations with transmitter-receiver great circle paths (TRGCPs) shown in Figure 1 cover low-equatorial-low-latitude region. To model D region ionosphere electron density variation, we have utilized long-wave propagation capability (LWPC; version 2.1) code (Ferguson, 1998). In LWPC modeling, observed amplitude and phase of a VLF signal are matched with the output from LWPC code by appropriately changing the input parameters. Subsequently, ionospheric electron density height profile is derived for the D region ionosphere by means of Wait's ionospheric parameters known as the reflection height (H') and the electron density sharpness factor parameter (β) (Wait & Spies, 1964), which are being used as input to LWPC code and provide best matching between the amplitude and phase outputs with their observed values.

LWPC code is described in section 3. Section 4.1 presents the observations of VLF signal during 22 July TSE, and section 4.2 presents LWPC modeling results and change in the *D* region electron density in the altitude range of 60–85 km. Finally, results are discussed in section 5 and summarized in section 6.

2. TSE Details and Data Set

TSE of 22 July 2009 started through a night-day transition phase from India at 00:51:00 UT and ended in the Pacific Ocean at ~04:20:00 UT. Totality trail was limited to 230-km belt, and partiality was seen much wider in the Indian subcontinent and in the far east Pacific region. Trail of the Moon's umbral shadow commenced from India and crossed in the course of time to Nepal, Bangladesh, Bhutan, Burma, and China. Subsequent to its passage from mainland Asia, the TSE totality trail touched the Ryukyu Islands in Japan and bent southeast all the way through to Pacific Ocean (Figure 1) with maximum totality period of 6 min 39 s (http://eclipse.gsfc.nasa.gov/SEmono/TSE2009/TSE2009.html; Espenak & Anderson, 2006).

In the present work, we have utilized observations of 19.8-kHz fixed frequency VLF signal from NWC transmitter located in the Australia (low-latitude region in the Southern Hemisphere). The NWC signal was recorded at three VLF receiver sites located in India at Allahabad (25.40°N, 81.93°E), Varanasi (25.30°N, 82.93°E), and Nainital (29.35°N, 79.45°E), one site located in South Korea at Busan (35.23°N, 129.08°E) and one site located in Fiji (low-latitude region in the Southern Hemisphere) at Suva (18.2°S, 178.4°E). The great circle paths of NWC signal originate from a southern low-latitude location and then cross southern equatorial region to the northern low-latitude and midlatitude stations (Figure 1).

The recording instrument used in India is an AWESOME VLF receiver (Cohen et al., 2010; Singh et al., 2010). At Busan, Sudden Ionospheric Disturbance (SID) monitor (Scherrer et al., 2008) and at Suva SoftPal (Kumar et al., 2008) VLF data recording systems were used. AWESOME and SoftPal data were recorded with 1-Hz sampling frequency, and SID monitor data were recorded at 12-Hz sampling frequency. But throughout our analysis, we have used 1-min average data from all stations.

3. LWPC Model

LWPC (version 2.1) code (Ferguson, 1998) has been used for model calculation of the amplitude and phase of observed NWC VLF signal at five sites on control day and day under TSE ionospheric conditions. LWPC code is adaptable code, which utilizes waveguide mode theory and considers region inside the ground and lower ionosphere as a waveguide known popularly as EIWG. The LWPC code utilizes two *D* region Wait parameters: H' (km) and β (km^{-1}) as inputs and gives output modeled amplitude and phase corresponding for a given TRGCP. The H' and β known as Wait parameters are extensively used to determine modeled electron density profile $N_e(z)$ for the *D* region between 60- and 100-km altitudes, which is given by the following equation as a function of altitude *z*. (Wait & Spies, 1964):

$$Ne(z) = 1.43 \times 10^7 \exp\left(-0.15 H'\right) \exp\left[(\beta - 0.15)\left(z - H'\right)\right] \text{ cm}^{-3} \tag{1}$$

In above equation (1), H' and β are the key parameters, which give altitude $N_e(z)$ profile and have been used by many workers to calculate *D* region electron density height profile using LWPC modeling of narrowband VLF observations (e.g., Clilverd et al., 2001; Guha et al., 2010; Han & Cummer, 2010a, 2010b; Kumar et al., 2016; Thomson et al., 2007). In the modeling process first, we model control day amplitude and phase of the VLF signal, which in this case is the NWC signal (19.8 kHz). To do so, we matched the observed amplitude and phase level with the output from LWPC code by choosing appropriate values of H' and β as input parameters. The each TRGCP is divided into different segments depending on the TRGCP path length from the transmitter to the receiver. The values of H' and β parameters are varied simultaneously (at an interval of 0.2 km for H' and 0.001 km^{-1} for β) until the output of LWPC matches with the observed amplitude and phase of VLF signal. This value of H' and β parameter is considered as control day value. Figures 2a and 2b show an example of LWPC modeling on 09 July 2009 (control day) for the daylight period (00–11 UT, or 5:30–15:30 LT) in Indian sector for the NWC VLF transmitter signal (19.8 kHz) recorded at Allahabad, India. The date of 9 July is chosen as a control day after considering the complete availability of data set and quiet geomagnetic conditions. The corresponding values of H' and β parameters for which a close
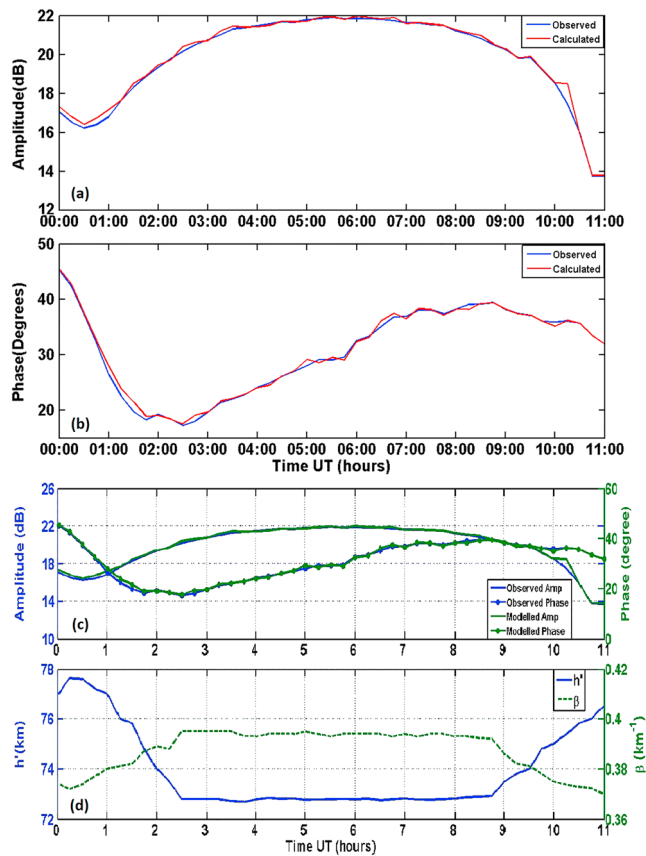
Figure 2. (a and b) A typical example of NWC (19.8 kHz) amplitude and phase observed at Allahabad and corresponding modeled amplitude and phase using long-wave propagation capability code. (c and d) Wait ionospheric parameters, H' and β as input to the long-wave propagation capability code corresponding to which modeled amplitude and phase were obtained that matched with observed amplitude and phase values.

match with observed amplitude and phase of NWC VLF signal is obtained are also presented as Figures 2c and 2d. In order to model the solar eclipse day VLF signal amplitude, we estimate the change in the VLF signal amplitude for respective TRGCPs on the eclipse day relative to the non-eclipse day (control day). The signal amplitude change or difference is further added to the respective normal time values of different TRGCPs; thus, perturbed signal is obtained. Subsequently, H' and β values corresponding to solar eclipse perturbed VLF signal amplitude are obtained by varying the H' and β values to match perturbed signal during TSE conditions.

4. Observations and Modeling

4.1. Observations of TSE Effect on NWC (19.8 kHz) VLF Signal

As shown in Figure 1, the TRGCPs of NWC signal to five stations of (1) Allahabad, (2) Varanasi, (3) Nainital, (4) Busan, and (5) Suva cover regions from no-eclipse to partiality to totality region in low and equatorial sectors. Further, all TRGCPs except NWC-Suva had almost perpendicular intersection alignment to the totality path (Figure 1). This forms a unique geometry of transmitter and receivers during TSE of 22 July 2009. Figures 3a–3c present variations of NWC signal during TSE conditions at stations in the Indian sector. The TRGCP distance from NWC transmitter located in Australia to three Indian stations (1) Allahabad (ALD), (2) Varanasi (VNS), and (3) Nainital (NAT) is around ~4,800 km (Figure 1). In India maximum eclipse with magnitude 1.015 was seen at VNS, followed by 1.001 at ALD, and NAT was in partial eclipse with magnitude 0.845. The total period of the eclipse in the Indian sector around three stations was from ~00–02 UT. On the eclipse day during 00–02 UT the geomagnetic conditions were quiet with K_p index between 1 and 3. But the eclipse event was immediately followed by a moderate geomagnetic storm with minimum D_{st} index value of −83 nT at 07:00 UT (source: http://wdc.kugi.kyoto-u.ac.jp/). Moderate geomagnetic storms have been found to have a negligible effect on the D region especially over low-latitude region (Kumar & Kumar, 2014; Peter et al., 2006).

The NWC signal amplitude variations for 3-hr duration (00:00–03:00 UT) for NWC-ALD, NWC-VNS, and NWC-NAT TRGCP on 22 July 2009 (red line) and control days (blue line) are presented in Figures 3a–3c. The vertical pink lines R1, R2, and R3 correspond to the start, maximum, and end of TSE at respective receiver stations. ALD station was in 100% totality and located on the fringe of totality path (Figure 1). At ALD station, the eclipse magnitude was 1.001 at the maximum of the eclipse at 00:55:31.4 UT and with totality duration of 45.6 s. ALD site observed the maximum decrease of 2.62 dB (Figure 3a) in the signal amplitude around totality maximum at ~00:55:31 UT, which returned to its normal level around the end of the eclipse at 01:56:46 UT. The amplitude decrease at ALD was maximum when compared to other all four observation sites. The VNS site was closer to the central line of totality (Figure 1) having larger eclipse magnitude of 1.015, and at this site a decrease in the signal amplitude observed was 1.98 dB (Figure 3b). The effect of eclipse was quite variable at NAT station where the eclipse coverage was ~85% with partial eclipse starting at 00:03:36 UT and ending at 01:56:19 UT. Initially, the amplitude increases of 2.17 dB occurred at 00:18:00 UT and recovered to its usual value at 00:27:10 UT, after that signal amplitude gradually decreased to a minimum of 2.34 dB at 00:57:12 UT (Figure 3c). Due to a technical problem with data recording at Nainital site on 21 and 23 July 2009, 24 July has been used as a control day.

Figure 3d presents the NWC signal variation on 22 July at an East Asian station, Busan, South Korea, of which TRGCP length is 6,532 km (Figure 1). Busan station was in 85% eclipsed region similar to Nainital station in the Indian sector and showed similar signal variation as Nainital with first an increase and then a decrease in the NWC amplitude. Pacific region station, Suva, Fiji, had a partial eclipse of 40%. It is
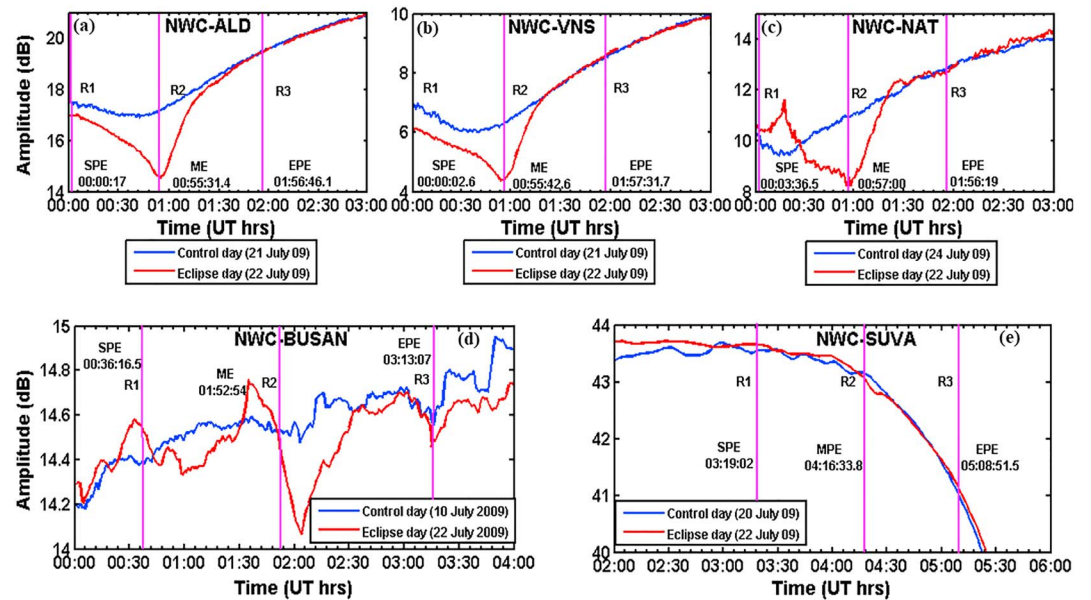
Figure 3. The amplitude variation of NWC (19.8 kHz) very low frequency signal at all five stations, (a) Allahabad (ALD), (b) Varanasi (VNS), (c) Nainital (NAT), (d) Busan, and (e) Suva, during a respective control day and on 22 July 2009 total solar eclipse day.

important to note from Figure 1 that more than ~85% of 6,678 km NWC-Suva TRGCP was in noneclipse region indicating a minimum influence of eclipse on NWC-Suva path.

The NWC signal variation at Suva shown in Figure 3e shows almost same type of signal variation both on eclipse and control days,

From NWC signal observations presented in Figures 3a–3d, it is evident that during a solar eclipse the structure of EIWG becomes incredibly variable, which in turn affects the interference pattern of the waveguide modes at the receiver and results in observed decrease/increase in the VLF signal amplitude. As observed, the decrease/increase in NWC amplitude in the Indian sector was different at different stations. The decrease in the amplitude occurred both at Allahabad and Varanasi stations, which were in the totality region. Maximum amplitude decrease occurred at Allahabad, which was located on the fringe of totality path. An increase and then a decrease in the signal amplitude occurred at Nainital and Busan sites, which were located in ~85% partial eclipse region. At Suva, in the Pacific region, almost no change in NWC signal variation was observed on eclipse day since its TRGCP was almost in the noneclipse region.

4.2. LWPC Modeling of Eclipsed Time NWC (19.8 kHz) VLF Signal

In order to qualitatively identify the changes observed in NWC VLF signal on 22 July 2009 (Figure 3), we applied LWPC code modeling to estimate the variations induced in the D region ionosphere reflection height and in the electron density. The methodology adopted for LWPC modeling has been elaborated in section 3. NWC VLF signal recorded at all the five stations and as presented in Figure 3 was modeled using LWPC (V2.1) code for a selected time period 00–03 UT. Subsequently, H' and β were varied to obtain good agreement between observed and modeled NWC VLF signal amplitude.

Table 1 presents the LWPC obtained variables H' and β for TSE and control days for all five stations for NWC signal observed at these sites. To precisely replicate D region with LWPC code, it is always desirable to encompass together both amplitude and phase data. In the present case different types of VLF receivers were used in all the three sectors of the eclipse, which had different modes of recording capabilities. Three Indian and a Fijian station used AWESOME and SoftPal VLF receivers, respectively, which have the capability to record both the amplitude and phase of the signal. In South Korea (Busan) the receiver used was SID monitor, which records only amplitude of the VLF signals. Further, it is important to mention that during July 2009 most of the time NWC phase data were irregular and of not good usable quality. Thus, in the present

Table 1
Summary of Change in Reference Height H′ (km) and the Exponential Sharpness Factor β (km^{-1}) Parameters as Observed Over Five TRGCP's on Respective Control Days and 22 July 2009 Eclipse Day

TRGCP	Control day		22 July 2009 eclipse day	
	H'(km)	β (km^{-1})	H' (km)	B (km^{-1})
NWC-ALD	77.0 (21 July)	0.38	80.0 [3.0] ↑	0.40 [0.02] ↑
NWC-VNS	78.5 (23 July)	0.34	80.7 [2.3] ↑	0.36 [0.02] ↑
NWC-NAT	77.0 (24 July)	0.36	80.0 [3.0] ↑	0.38 [0.02] ↑
NWC-BUSAN	70.0 (12 July)	0.43	72.4 [2.4] ↑	0.44 [0.01] ↑
NWC-SUVA	71.0 (20 July)	0.34	71.0 [0.0]	0.34 [0.0]

Note. ALD = Allahabad; BUSAN = Busan; NAT = Nainital; SUVA = Suva; TRGCP = transmitter-receiver great circle path; VNS = Varanasi.

work, we have used only NWC amplitude for all stations. In the absence of phase data, different sets of H' and β values are possible for a given amplitude value. In order to get the unique values of H' and β with only amplitude data, we have selected most appropriate set of H' and β after several iterations of LWPC code, which very closely matched with the observed VLF signal. In order to validate chosen values of H' and β from LWPC code for perturbed amplitude, we have used similar method as used by many other workers in absence of good phase data (Guha et al., 2012; Maurya et al., 2014; Phanikumar et al., 2014). The final values of H' and β obtained for the VLF variations due to 22 July TSE are presented in Table 1.

From Table 1 it is significant to note that for NWC TRGCPs to the sites of ALD, VNS, NAT, and BUSAN located in and around totality path, an increase in parameters H' and β on TSE day was estimated when compared to respective control days. The modeling of NWC signal observed at ALD, which was located on the fringe of totality path, yielded the H' and β as 80.0 km and 0.40 km^{-1} which when compared with ALD control day H' and β of 77.0 km and 0.38 km^{-1}, respectively, gives an increase in H' of 3.0 km and in β of 0.02 km^{-1}. Correspondingly, at VNS station, which was also located near the central line of totality path, H' and β increased by 2.3 km and 0.02 km^{-1}, respectively. Nainital and Busan, which were in 85% obscuration (partial eclipse area), the increase in H' and β was 3.0 km, 2.4 km, and 0.02 km^{-1}, 0.01 km^{-1}, respectively. On NWC-SUVA TRGCP no change in H' and β was observed as expected since most of part of TRGCP was in the noneclipse region as evident from Figure 1. LWPC modeled output of H' and β as presented in Table 1 for control and eclipse day clearly shows increase in the VLF reference height and the sharpness of EIWG by July 2009 TSE.

Modeling of VLF signal shows that influence of TSE on the NWC signal received at the sites located at the fringe and near central line of totality path and under 85% obscuration varied considerably. The H' varied from 2.3 km near central line of totality to 3.0 km at the fringe of totality path and 2.4 and 3.0 km in 85% partial eclipse region. Next, we compare our LWPC model results of H' and β with the only available report of comprehensive modeling D region ionosphere in European sector midlatitude and high-latitude regions (Clilverd et al., 2001) for 11 August 1999 TSE. Scrutinizing the VLF signal for 14 TRGCPs with great circle path in the range of >1,000 to <10,000 km, Clilverd et al. (2001) demonstrated a change of ~1 dB in VLF amplitude corresponds to a modification of $H' = 1.1$ km and $\beta = 0.01$ km^{-1}. In the present case of 22 July 2009 TSE, signal TRGCPs were mostly in the low and equatorial regions and maximum increase in the H' and β observed was 3.0 km and 0.02 km^{-1}, respectively. Therefore, 22 July 2009 TSE study compared with 11 August 1999 TSE shows variable TSE effects on the ionosphere, probably due to different ionospheric dynamics in different latitude regions of the globe, the different interaction of TRGCPs with eclipse paths, and different times of TSE occurrence. Hence, it is important to understand the effect of TSE on Earth's ionosphere over different sectors of the globe under different daytime conditions. The present results show that during a TSE, an increase in the H' and β is more in the low-latitude region when compared with the midlatitude region (Clilverd et al., 2001).

LWPC model obtained H' and β presented in Table 1 show increase in the H' on TSE day. Using LWPC obtained H' and β several workers have used conventional Wait profile (Wait & Spies, 1964) to create D region electron density profiles, $N_e(h)$ in per cubic centimeter up to altitude of 100 km under normal and
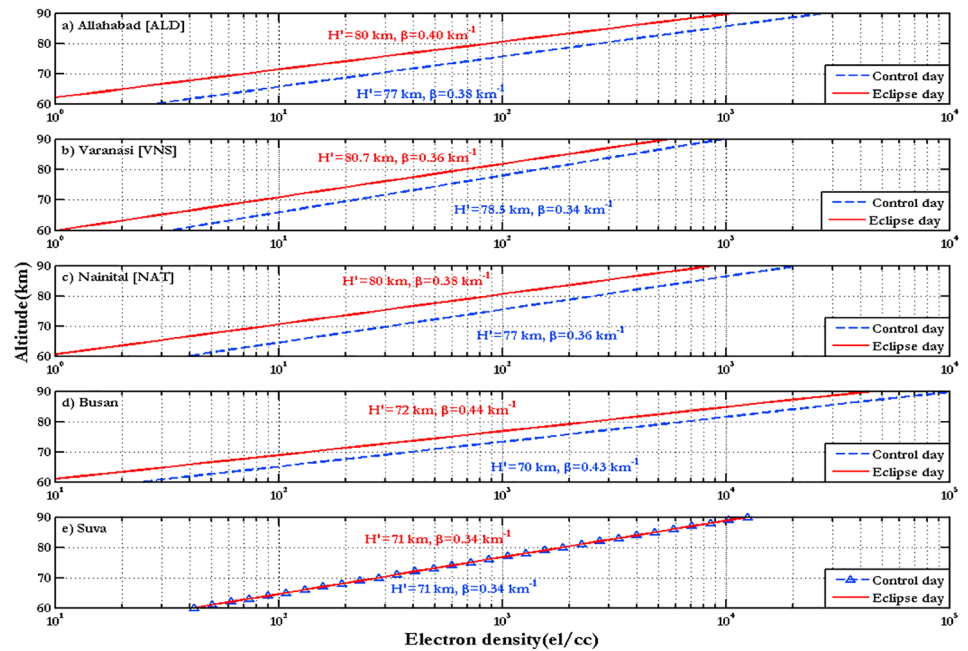
Figure 4. Vertical profile of D region electron density in the altitude range 60–85 km on respective control day and on 22 July 2009 total solar eclipse day at all five stations, (a) Allahabad (ALD), (b) Varanasi (VNS), (c) Nainital (NAT), (d) Busan, and (e) Suva.

perturbed geophysical conditions (e.g., Kumar et al., 2015; McRae & Thomson, 2004; Thomson et al., 2005). Figures 4a–4e present the $N_e(h)$ at all the five stations: ALD, VNS, NAT, BUSAN, and SUVA obtained using equation (1), wherein values of input parameters H' and β were taken from Table 1 on respective control days and on 22 July TSE day. At Suva (Figure 4e), the overlapping of control and eclipse day green line profile represents no change in the electron density in the altitude range 60–85 km. The result is understandable since the NWC-SUVA TRGCP did not see any considerable effect of the eclipse. It must be noted that N_e profile shown in Figure 4 for control days and reduction in N_e on 22 July 2009 TSE day at four sites, ALD, VNS, NAT, and BUSAN, is not a reduction of N_e in solar eclipse affected segment of TRGCP; rather, it is an average decrease in N_e all along the whole TRGCP (Kumar et al., 2015) that would cause the same changes in the H' and β as estimated in this study. Considering 75-km altitude as the daytime D region reference height, we next compare N_e profiles presented in Figure 4 on control and TSE days. ALD site (Figure 4a) was located on the fringe of totality path where the totality occurred for about 45.4 s and N_e at 75-km altitude decreased to 25.2×10^2 cm^{-3} on TSE day when compared to control day values of 87.0×10^2 cm^{-3} which is about 71% decrease from the normal value. Similarly, VNS site (Figure 4b) located near central line of totality path experienced longer totality duration of ~3 min 03 s and showed about 58% decrease in the N_e at 75 km with 23.89×10^2 cm^{-3} N_e on TSE day and 56.58×10^2 cm^{-3} on the control day. Hence, the decrease in N_e on TSE day was more over NWC-ALD TRGCP (~71%) terminating at the fringe of totality line compared to NWC-VNS TRGCP (~58%), which was terminating near the line of totality. The two other stations NAT (in Indian sector) and BUSAN (in east Asian sector), which were under the influence of ~85% partiality, experienced a decrease in N_e of ~69% and ~63%, respectively, at 75-km altitude on TSE day (Figures 4c and 4d).

5. Discussion

We have analyzed and modeled 22 July 2009 TSE effect on the VLF propagation and the D region iono-sphere in the low and equatorial regions using the NWC (19.8 kHz) VLF transmitter signal recorded at five stations. Five stations covered whole eclipse region from the start of the eclipse in India to its end in the Pacific Ocean. The 22 July 2009 TSE was one of the most studied TSEs of the recent decade. In

terms of maximum totality duration, it was much longer (6 min 39 s) than very recent great American TSE of 21 August 2017 (2 min 40 s). It is well known that during a TSE due to blockage of solar ionizing radiation (Lyman-α, 1,215 Å) by the Moon during totality period creates nighttime like situation and decrease in the electron density of entire ionosphere below the shadow region. However, during a TSE ionospheric electron density is larger than that of nighttime values because some ionization is still produced by means of soft X-ray and extreme ultraviolet emissions coming from the limb solar corona (e.g., Curto et al., 2006; Guha et al., 2010, 2012; Maurya et al., 2014; Ohya et al., 2012; Phanikumar et al., 2014; Singh et al., 2011; Singh et al., 2012).

TSE effect is more prominently noticeable in the D region as the electron density decreases and reaches close to nighttime values. A decrease in the electron density results in an increase in the D region reflection height and hence creates a discontinuity in the EIWG. This changes the propagation condition for the VLF waves and can generate VLF signal anomaly. Now the interesting science questions are the following: What is the magnitude of VLF anomaly (positive/negative or increase/decrease)? Is observed VLF anomaly same in different latitude-longitude sectors. What are the factors/parameters controlling it? Answers of these questions require study of different TSE cases with various combinations of TRGCPs and eclipse timings and characteristics. The present study is an attempt to answer these questions by using VLF data recorded at five stations located in low-equatorial-low-latitude region during 22 July 2009 TSE and compare the results with past TSE observations and report new results.

There have been previous reports on 22 July 2009 TSE effect on the D region ionosphere. Guha et al. (2010) reported a decrease in the VLF signal amplitude from VTX (18.2 kHz) transmitter located in India and recorded at an Indian station, Tripura, with TRGCP path length ~2,350 km. The transmitter (VTX) and receiver (Tripura) were in ~74% and ~90% of totality. Guha et al. (2010) reported a decrease of 3.2 dB in VTX amplitude on TSE day compared to a normal day. In another report on 22 July TSE, Phanikumar et al. (2014) for very short TRGCP path length (~390 km) from JJI (22.2 kHz) VLF transmitter signal from Japan (~95% eclipse) to a station Busan (85% of totality), South Korea, observed a decrease in the JJI signal amplitude of ~6.2 dB. The decrease in the VLF signals amplitude reported by Guha et al. (2010) and Phanikumar et al. (2014) is similar to present observations of the amplitude decrease in NWC (19.8 kHz) signal at Allahabad, Varanasi, Nainital, and Busan receiving stations near totality/maximum eclipse time. For the stations like Nainital and Busan, which were in the partial eclipse condition, first an increase in the VLF amplitude at the beginning of eclipse followed by the amplitude recovery was observed with a maximum decrease near the maximum of the eclipse. The trend of maximum decrease in the VLF signal amplitude in previous reports and present study is observed near the time of maximum eclipse at respective stations. The magnitude of decrease in the amplitude in previous reports and in the present study is different, which is probably due to different TRGCP path lengths and time of the eclipse maximum. The amplitude decrease of ~6.2 dB found by Phanikumar et al. (2014) for the very short path (~390 km) is maximum till now reported when compared to any report on 22 July 2009 TSE. In our study, all TRGCPs were in north-southeastern orientation, almost perpendicular to the totality path.

Observations suggest that during a TSE magnitude of VLF signal amplitude decrease depends on TRGCP path length and its orientation with totality path, time of eclipse, and the eclipse magnitude. The only exception of signal amplitude increase was reported by Maurya et al. (2014) for the TRGCPs parallel to totality path. Maurya et al. (2014) investigated eclipse induced wave-like signatures (WLSs) in D region ionosphere using JJI (22.2 kHz) VLF transmitter in Japan of which TRGCP to receiving stations in the Indian sector was parallel to totality path. Maurya et al. (2014) found only increase in the amplitude at Allahabad and Varanasi, contrary to present observations of the amplitude decrease of NWC signal whose TRGCP is perpendicular to the totality path. Busan and Fiji stations also showed a decrease in the amplitude near partial eclipse (Maurya et al., 2014). Nainital site with partial eclipse presents a unique case where we observed almost similar change in the NWC signal amplitude with the first increase and then decrease as in the case of Maurya et al. (2014) for JJI signal. But it is important to mention here that in the work of Maurya et al. (2014) at Nainital site, the TSE effect on JJI (22.2 kHz) signal amplitude was more pronounced as the amplitude minima occurred close to the maximum of the eclipse at JJI transmitter. Whereas in the present case with NWC (19.8 kHz) signal, amplitude minima at Nainital (receiving station) is seen close to maximum eclipse time at Nainital.

Overall, with above discussion, it can be summarized that the decrease/increase in VLF amplitude signal mostly depends on the path length and orientation of TRGCP with totality path. As our results are limited with only one solar eclipse, therefore, we suggest further investigations with more TSEs with various combinations of TRGCPs, if there is such an opportunity in the future.

Now we discuss our results with most comprehensive work done by Clilverd et al. (2001) for 11 August 1999 TSE in the European sector. For very short path length (<500 km), they observed both increase and decrease in the amplitude of GBZ, GBR, and FTA2 VLF transmitters received at Cambridge station. Whereas for short path (<2,000 km) an increase in the amplitude was observed for FTA2-Saint Ives; FTA2-Saint Wolfgang; DHO-Saint Wolfgang; DHO-Budapest; GBR-Saint Wolfgang; GBR-Budapest, and GBZ-Budapest TRGCPs and for long path length (>10,000 km) a decrease in the VLF signal amplitude was found for FTA2-Halley, GBZ-Halley; GBR-Halley, and DHO-Halley TRGCPs. For other cases (medium path length TRGCP >2,000 and <10,000 km) mixed results were reported. In the present case, we have all five TRGCPs of medium path length (>2,000 and <10, 000 km), but we observed only decrease in the VLF signal amplitude. Though we have seen an initial increase (e.g., Nainital and Busan), but major eclipse effect was a decrease in the VLF amplitude near the time of eclipse maximum. It is important to note that in the present case all TRGCPs were aligned in the north-southeastern or near perpendicular direction to the totality path and confined in low-equatorial-low-latitude region. This may be a probable reason why we observed only decreases in the VLF signal amplitude on TRGCPs of medium path lengths.

Present observations of TSE time NWC (19.8 kHz) signal variations are important when we compare especially with that of Maurya et al. (2014) investigation of eclipse induced WLSs in the D region ionosphere. Maurya et al. (2014) used the signal from JJI (22.1 kHz) VLF transmitter located in Japan whose TRGCPs to Indian stations were parallel to totality path. Maurya et al. (2014) found an increase in JJI signal amplitude at Allahabad and Varanasi stations, contrary to present observations. At Nainital station, which was in partial eclipse, almost similar signature of first an increase and then a decrease in the amplitude was observed as in the case of Maurya et al. (2014). Hence, we observe that for stations located in totality path and with TRGCP alignment parallel to the totality path there is an increase in received VLF signal amplitude (Maurya et al., 2014) due to reduced attenuation created by nighttime like conditions, whereas in the present study a decrease in the VLF amplitude was observed when TRGCP intersection was perpendicular to totality path due to modal interference at the receivers created by the discontinuity in the EIWG by the TSE. Further important finding of Maurya et al. (2014) is the detection of WLS during the eclipse at stations ALD, VNS, NAT, and BUSAN. Maurya et al. (2014) using Mother wavelet analysis showed the existence of WLS with period ~16–40 min at Allahabad and Varanasi stations located beneath totality region, and ~30- to 80-min period at Nainital and Busan beneath partial eclipse. They suggested that WLS are most likely induced by the ionospheric electron density changes (gradient) due to atmospheric gravity waves (AGWs) associated with 22 July 2009 TSE. The N_e profile in the altitude range 60–85 km on TSE and control days presented in Figure 4 seems a step toward explaining the WLS in D region ionosphere during a TSE created by the combination of reduction in the ionization and AGWs created by the supersonic motion of cooling spot of TSE in the stratosphere (Chimonas, 1970; Chimonas & Hines, 1970).

Normally the sunlit D region is steady with about no temporal changeability in the electron density gradients. But during a solar eclipse, the supersonic movement of eclipse cooling spot at ~45-km altitude in stratosphere perturbs the heat equilibrium of atmosphere and is considered as most important cause of AGWs (Chimonas, 1970; Chimonas & Hines, 1970; Gerasopoulos et al., 2008). The AGWs propagate outward and upward and can cause traveling ionospheric disturbances (Chen et al., 2011; Vlasov et al., 2011). These TSE time AWGs originated at stratospheric altitudes have major implications on the middle atmosphere and lower ionosphere (10–110 km) because of declining atmospheric density with height due to which the amplitude of AGWs increases with the altitude. It is now well known that AGWs in lower atmosphere and WLS in ionosphere are caused by abrupt transformation in solar flux, temperature, electron density, plasma conductivity, and plasma instability during nighttime, night/day and day/night transition times and by rare astronomical events like solar eclipses (Maurya et al., 2014; Somsikov & Ganguly, 1995).

The observations and modeling of D region ionosphere during 22 July 2009 TSE results presented in Figure 4 show that for the region near to the central line of totality the plasma depletion is less when compared to regions away from the line of totality. A 58% depletion in N_e at Varanasi near central line of totality, 71%

at Allahabad on the fringe of totality, 69% and 63% depletion at NAT and Busan stations in partial eclipse, was estimated using LWPC modeling of signal anomalies. Further, when we compare our D region ionosphere modeling results of 22 July 2009 solar eclipse with the eclipse of 11 August 1999 eclipse in the European sector for which modeling was done by Clilverd et al. (2001) and reported ~80% drop in electron concentration at 77 km. Present results indicate that during a TSE in low-equatorial-low latitude region decrease in the D region electron density is less (~70%) when compared with TSE time decrease in D region electron density (~80%) in midlatitude to high-latitude region as reported by Clilverd et al. (2001). However, this statement is not conclusive as we need more studies of TSE time D region ionosphere to come to any conclusion and due to uncertainties in the observations and modeling limitations.

6. Summary

In the present work on the D region ionosphere perturbations during 22 July 2009 TSE, we used NWC (19.8 kHz) VLF signal recorded at five stations located in India, South Korea, and Fiji. The TRGCPs of NWC signal to these stations were almost perpendicular to the totality path, and signal propagation was confined in low-equatorial-low-latitude regions. This is the only comprehensive report using wider database, which studied the response of D region ionosphere for an eclipse in the low-latitude region. The new results found from the observations and LWPC modeling have been discussed in comparison with several previous TSE works. The outcome of the study is mainly compared with comprehensive TSE time LWPC modeling results of Clilverd et al. (2001) for 11 August 1999 TSE in the midlatitude European sector. The unique findings of the present study are summarized as follows:

1. The ionospheric reflection height H' increased differently at different stations located in the different strengths of totality of 22 July 2009 TSE. The H' increased by 2.3 km at the station (Varanasi) near central line of totality, by 3.0 km at the station (Allahabad) located in the fringe of totality path, by 2.4 km at station Nainital, and by 3.0 km at station Busan located in 85% of the totality (partial eclipse region).
2. Observations and modeling results show that during 22 July TSE the increase in the H' and β is more in the low-latitude region when compared with midlatitude (Clilverd et al., 2001). The increase in H' and β for 22 July TSE in low latitude was 3.0 km and 0.02 km^{-1}, respectively, and for midlatitude the increase in was 1.1 km and 0.01 km^{-1}, respectively, for 11 August 2011 TSE (Clilverd et al., 2001).
3. Wait ionospheric profile using H' and β in the altitude range 60–85 km for 22 July TSE in low-latitude region showed a reduction in the D region electron density of about 70%, which is less when compared with TSE time electron density reduction of about 80% in midlatitude region for 11 August 2011 TSE (Clilverd et al., 2001).
4. Considering 75-km altitude as the daytime reference height of D region ionosphere, reduction in electron density observed was about 58% at the station Varanasi near the central line of totality. At Allahabad, station in the fringe of totality line, the decrease in the electron density was about 71%. At stations, Nainital and Busan in partial eclipse, the density reduction was 69% and 63%, respectively. Hence, reduction in D region electron density during TSE near the central line of totality is less as compared to the locations away from totality central line.

References

Baran, L. W., Ephishov, I. I., Shagimuratov, I. I., Ivanov, V. P., & Lagovsky, A. F. (2003). The response of the ionospheric total electron content to the solar eclipse on 11 August 1999. *Advances in Space Research*, *31*(4), 989–994. https://doi.org/10.1016/S0273-1177(02)00885-2

Chen, G., Zhao, Z., Zhang, Y., Yang, G., Zhou, C., Huang, S., Li, T., et al. (2011). Gravity waves and spread Es observed during the solar eclipse of 22 July 2009. *Journal of Geophysical Research*, *116*, A09314. https://doi.org/10.1029/2011JA016720

Chimonas, G. (1970). Internal gravity-wave motion induced in the Earth's atmosphere by a solar eclipse. *Journal of Geophysical Research*, *18*, 5545–5551. https://doi.org/10.1029/GM018p0708

Chimonas, G. C., & Hines, O. (1970). Atmospheric gravity waves induced by a solar eclipse. *Journal of Geophysical Research*, *75*, 857–875. https://doi.org/10.1029/JA075i004p00875

Clilverd, M. A., Rodger, C. J., Neil, R. T., Lichtenberger, J., Steinbach, P., Cannon, P., & Angling, M. J. (2001). Total solar eclipse effects on VLF signals: Observation and modeling. *Radio Science*, *36*, 773–788. https://doi.org/10.1029/2000RS002395

Cohen, M. B., Inan, U. S., & Paschal, E. W. (2010). Sensitive broadband ELF/VLF radio reception with the AWESOME instrument. *IEEE Transactions on Geoscience and Remote Sensing*, *48*(1), 3–17. https://doi.org/10.1109/TGRS.2009.2028334

Cummer, S. A., & Inan, U. S. (2000). Ionospheric E region remote sensing with ELF radio atmospherics. *Radio Science*, *35*, 1437–1444. https://doi.org/10.1029/2000RS002335

Curto, J. J., Heiig, B., & Pinol, M. (2006). Modeling the geomagnetic effects caused by solar eclipse of 11 August 1999. *Journal of Geophysical Research*, *111*, A07312. https://doi.org/10.1029/2005JA011499

Espenak, F., & Anderson, J. (2006). Predictions for the total solar eclipses of 2008, 2009, and 2010. In *Proceedings IAU Symposium No. 233, Solar Activity and its Magnetic Origin*, (pp. 495–502). Cambridge: Cambridge University Press. https://doi.org/10.1017/S1743921306002547

Ferguson, J.A. (1998). Computer programs for assessment of long-wavelength radio communications, Version 2.0: User's Guide and Source Files, No. TD-3030, Space and Naval Warfare Systems Center, San Diego, CA.

Gerasopoulos, E., Zerefos, C. S., Tsagouri, I., Founda, D., Amiridis, V., Bais, A. F., Belehaki, A., et al. (2008). The total solar eclipse of March 2006: Overview. *Atmospheric Chemistry and Physics*, *8*(17), 5205–5220. https://doi.org/10.5194/acp-8-5205-2008

Guha, A., De, B. K., Choudhury, A., & Roy, R. (2012). Spectral character of VLF sferics propagating inside the Earth ionosphere waveguide during two recent solar eclipses. *Journal of Geophysical Research*, *117*, A04305. https://doi.org/10.1029/2011JA017498

Guha, A., De, B. K., Roy, R., & Choudhury, A. (2010). Response of the equatorial lower ionosphere to the total solar eclipse of July 22, 2009 during sunrise transition period studied using VLF signal. *Journal of Geophysical Research*, *115*, A11302. https://doi.org/10.1029/2009JA015101

Han, F., & Cummer, S. A. (2010a). Midlatitude nighttime D region ionosphere variability on hourly to monthly timescales. *Journal of Geophysical Research*, *115*, A09323. https://doi.org/10.1029/2010JA015437

Han, F., & Cummer, S. A. (2010b). Midlatitude daytime D region ionosphere variations measured from radio atmospherics. *Journal of Geophysical Research*, *115*, A10314. https://doi.org/10.1029/2010 JA0 15715

Hargreaves, J. K. (1992). *The solar-terrestrial environment*. New York: Cambridge University Press. https://doi.org/10.1017/CBO9780511628924

Kumar, A., & Kumar, S. (2014). Space weather effects on the low latitude D-region ionosphere during solar minimum. *Earth, Planets and Space*, *66*(1), 76–77. https://doi.org/10.1186/1880-5981-66-76

Kumar, S., Kumar, A., Maurya, A. K., & Singh, R. (2016). Changes in the D region associated with three recent solar eclipses in the South Pacific region. *Journal of Geophysical Research: Space Physics*, *121*, 5930–5943. https://doi.org/10.1002/2016JA022695

Kumar, S., Kumar, A., Menk, F., Maurya, A. K., Singh, R., & Veenadhari, B. (2015). Response of the low-latitude D region ionosphere to extreme space weather event of 14–16 December 2006. *Journal of Geophysical Research: Space Physics*, *120*, 788–799. https://doi.org/10.1002/2014JA020751

Kumar, S., Kumar, A., & Rodger, C. J. (2008). Subionospheric early VLF perturbations observed at Suva: VLF detection of red sprites in the day? *Journal of Geophysical Research*, *113*, A03311. https://doi.org/10.1029/2007JA012734

Maurya, A. K., Phanikumar, D. V., Singh, R., Kumar, S., Veenadhari, B., Kwak, Y.-S., Kumar, A., et al. (2014). Low-mid latitude D region ionospheric perturbations associated with 22 July 2009 total solar eclipse: Wave-like signatures inferred from VLF observations. *Journal of Geophysical Research: Space Physics*, *119*, 8512–8523. https://doi.org/10.1002/2013JA019521

Maurya, A. K., Veenadhari, B., Singh, R., Kumar, S., Cohen, M. B., Selvakumaran, R., Gokani, S., et al. (2012). Nighttime D region electron density measurements from ELF-VLF tweek radio atmospherics recorded at low latitudes. *Journal of Geophysical Research*, *117*, A11308. https://doi.org/10.1029/2012JA017876

Maurya, A. K., Venkatesham, K., Kumar, S., Singh, R., Tiwari, P., & Singh, A. K. (2018). Effects of St. Patrick's Day geomagnetic storm of March 2015 and of June 2015 on low-equatorial D region ionosphere. *Journal of Geophysical Research: Space Physics*, *123*, 6836–6850. https://doi.org/10.1029/2018JA025536

McRae, W. M., & Thomson, N. R. (2004). Solar flare induced ionospheric D-region enhancement from VLF phase and amplitude observations. *Journal of Atmospheric and Solar - Terrestrial Physics*, *66*(1), 77–87. https://doi.org/10.1016/j.jastp.2003.09.009

Ohya, H., Tsuchiya, F., Nakata, H., Shiokawa, K., Miyoshi, Y., Yamashita, K., & Takahashi, Y. (2012). Reflection height of daytime tweek atmospherics during the solar eclipse of 22 July 2009. *Journal of Geophysical Research*, *117*, A11310. https://doi.org/10.1029/2012JA018151

Peter, W. B., Chevalier, M. W., & Inan, U. S. (2006). Perturbations of midlatitude subionospheric VLF signals associated with lower ionospheric disturbances during major geomagnetic storms. *Journal of Atmospheric and Solar - Terrestrial Physics*, *111*, A03301. https://doi.org/10.1029/2005JA011346

Phanikumar, D. V., Kwak, Y. S., Patra, A. K., Maurya, A. K., Singh, R., & Parke, S. M. (2014). Response of the mid-latitude D-region ionosphere to the total solar eclipse of 22 July 2009 studied using VLF signals in South Korean peninsula. *Advances in Space Research*, *54*(6), 961–968. https://doi.org/10.1016/j.asr.2014.06.005

Reeve, C. D., & Rycroft, M. J. (1972). The eclipsed lower ionosphere as investigated by natural very low frequency radio signals. *Journal of Atmospheric and Solar - Terrestrial Physics*, *3*, 667–672.

Scherrer, D., Cohen, M., Hoeksema, T., Inan, U., Mitchell, R., & Scherrer, P. (2008). Distributing space weather monitoring instruments and educational materials worldwide for IHY 2007: The AWESOME and SID project. *Advances in Space Research*, *42*(11), 1777–1785. https://doi.org/10.1016/j.asr.2007.12.013

Singh, A. K., Singh, R., Veenadhari, B., & Singh, A. K. (2012). Response of low latitude D-region ionosphere to the total solar eclipse of 22 July 2009, as deduced from ELF/VLF analysis. *Advances in Space Research*, *50*(10), 1352–1361. https://doi.org/10.1016/j.asr.2012.07.005

Singh, R., Veenadhari, B., Cohen, M. B., Pant, P., Singh, A. K., Maurya, A. K., Vohat, P., et al. (2010). Initial results from AWESOME VLF receivers: Setup in low latitude Indian region under IHY2007/UNBSSI program. *Current Science*, *98*(3), 398–405.

Singh, R., Veenadhari, B., Maurya, A. K., Cohen, M. B., Kumar, S., Selvakumaran, R., Pant, P., et al. (2011). D-region ionosphere response to the total solar eclipse of 22 July 2009 deduced from ELF-VLF tweek observations in the Indian sector. *Journal of Geophysical Research*, *116*, A10301. https://doi.org/10.1029/2011JA016641

Smith, L. G. (1972). Rocket observations of solar UV radiation during the eclipse of 7 March 1970. *Journal of Atmospheric and Solar - Terrestrial Physics*, *34*(4), 601–611. https://doi.org/10.1016/0021-9169(72)90147-X

Somsikov, V. M., & Ganguly, B. (1995). On the formation of atmospheric inhomogeneities in the solar terminator region. *Journal of Atmospheric and Solar - Terrestrial Physics*, *57*(12), 1513–1523. https://doi.org/10.1016/0021-9169(95)00014-S

Thomson, N. R., Clilverd, M. A., & McRae, W. M. (2007). Nighttime D region parameters from VLF amplitude and phase. *Journal of Geophysical Research*, *112*, A07304. https://doi.org/10.1029/2007JA012271

Thomson, N. R., Rodger, C. J., & Clilverd, M. A. (2005). Large solar flares and their ionospheric D region enhancements. *Journal of Geophysical Research*, *110*, 6306. https://doi.org/10.1029/2005JA0011008

Vlasov, A., Kauristie, K., Van de Kamp, M., Luntama, J. P., & Pogoreltsev, A. (2011). A study of traveling ionospheric disturbances and atmospheric gravity waves using EISCAT Svalbard radar IPY-data. *Annales Geophysicae*, *29*(11), 2101–2116. https://doi.org/10.5194/angeo-29-2101-2011

Wait, J. R., & Spies, K. P. (1964). *Characteristics of the Earth-ionosphere waveguide for VLF radio waves, Tech. Note* 300, Natl. Bur. of Stand., Boulder, CO.

Zhang, X.-F., Du, R. Y., Gu, S.-M., Wu, T., & Wang, Y.-N. (2011). Anomalous variation of VLF signals in the total solar eclipse of 22 July 2009. *Chinese Astronomy and Astrophysics*, *35*(1), 54–61. https://doi.org/10.1016/j.chinastron.2011.01.007